

The role of ergodicity and mixing in the central limit theorem for Casati-Prosen triangle map variables

Sílvia M. Duarte Queirós¹

Unilever R&D Port Sunlight, Quarry Road East, Wirral, CH63 3JW UK

(10th December 2008)

Abstract

In this manuscript we analyse the behaviour of the probability density function of the sum of N deterministic variables generated from the triangle map of Casati-Prosen. For the case in which the map is both ergodic and mixing the resulting probability density function quickly concurs with the Normal distribution. When these properties are modified the resulting probability density functions are described by power-laws. Moreover, contrarily to what it would be expected, as the number of added variables N increases the distance to Gaussian distribution increases. This behaviour goes against standard central limit theorem. By extrapolation of our finite size results we preview that in the limit of N going to infinity the distribution has the same asymptotic decay as a Lorentzian (or a $q = 2$ -Gaussian).

1 Introduction

The central limit theory has been a subject of studied within the natural sciences for many generations. We might even state that CLT originated in 1713 with Bernoulli's weak law of large numbers [1]. After Bernoulli, de Moivre [2], Laplace [3], and Gauss, amongst others, made crucial contributions to the establishment of the Normal probability density function (PDF) as the stable distribution when one considers the sum of independent and identically distributed random variables with finite standard deviation. The stability of the Normal distribution, the central limit theorem (CLT), was just formally established by the Russian mathematician Lyapunov 188 years after Bernoulli [4]. Afterwards, Lévy and Gnedenko [5, 6] generalised the CLT to account for independent and identically distributed random variables but with infinite standard deviations, followed by broader generalisations which include dependency between variables [7, 8]. With the advent of computation in the 1970s, chaos theory and non-linear phenomena achieved huge progress. It was then possible to verify the existence of a central limit theory for deterministic variables as well [9, 10]. More recently, central limit theory has been the focus of renewed interest within statistical mechanics mostly because of the endeavour to establish the optimising PDF of non-additive entropy S_q [11] as the stable distribution for the sum of random or deterministic variables for some special kind of correlation [12], on the edge of chaos [13, 14], or even for systems in a metastable state [15].

In the sequel of this manuscript we communicate results on numerical investigations of the distribution of deterministic variables which arise from the sum of variables generated

¹email address: Silvio.Queiros@unilever.com, sdqueiro@gmail.com

from the triangle map introduced by Casati and Prosen [16]. Our analysis is performed at two different regimes: a first illustrative one, for which the system is both *ergodic* and *mixing*, and a second in which the system is *weakly ergodic* and apparently *weakly mixing*². In the former case, the convergence towards the Gaussian distribution is clear and easily explained according to the standard CLT. In the latter case, we detect an anomalous behaviour characterised by non-Gaussian distributions which become more distant from the Gaussian distribution as the number of variables added increases. If we take into account the behaviour shown for phase occupancy observables in other conservative dynamical systems, this result is against all odds and it emphasises the very particular properties of this dynamical system. The remaining of the manuscript is organised as follows: in Sec. 2 we introduce the triangular map and some of its properties, and in Sec. 3 we present our numerical results. Some conclusions and remarks are made in Sec. 4.

2 The triangle map

The triangle map, $z_{t+1} = T(z_t)$ introduced by Casati and Prosen [17, 16], corresponds to a discrete transformation on a torus $z = (x, y) \in [-1, 1) \times [-1, 1)$ with symmetrical coordinates,

$$\begin{cases} x_{n+1} &= x_n + y_{n+1} \pmod{2} \\ y_{n+1} &= y_n + \alpha \operatorname{sign} x_n + \beta \pmod{2} \end{cases}, \quad (1)$$

where $\operatorname{sign} x = \pm 1$, and α and β are real parameters of the map. Function $\pmod{2}$ represents a modified definition of $\bmod 2$ in the interval between -1 and $+1$. This map has emerged from studies on the compatibility between linear dynamical instability and the exponential decay of Poincaré recurrences. Map (1) is parabolic and area preserving. For the Jacobian matrix we have, $\det J = 1$, and its trace, $\operatorname{Tr} J = 2$.

Concerning the relevance of parameters α and β , it is known that when both of the parameters are irrational numbers, the map is ergodic [16]. Moreover, it attains the ergodicity property, *i.e.*, averages over time equal averages over samples, very rapidly. For such a set of values the map is also *mixing* [17] in the sense that it has a *continuous spectral density* besides the property previously defined. Evaluating Poincaré recurrences, it has been found that the probability of an orbit to stay outside a specific subset of the torus for a time longer than t behaves as $\exp[-\mu t]$, with μ being very close to the Lesbegue measure of that subset. This fact is in accordance with a completely stochastic dynamics. The exponential decay leads to a linear separation of close orbits which has been related to non-extensive statistical mechanics formalism via a generalised Pesin-like identity that bridges a q -generalisation of Kolmogorov-Sinai entropy [19] and a q -Lyapunov coefficient from the sensitivity to initial conditions [20]. The entropic index of this map was found to be $q = 0$ [21].

²By *strongly ergodic* we mean systems for which the exploration rate $r(t) = n(t)/N$ [$n(t)$ is the number of cells visited by an orbit until a discrete time t and N is the total number of cells ($N \rightarrow \infty$)], averaged over several initial conditions, presents the same functional form as the exploration rate of a random model $r_{RM}(t) = 1 - \exp[-t/N]$. Concomitantly, by *strongly mixing* we refer to systems whose correlation function, $C(t)$ decays much faster than $t^{-\mu}$ with $\mu \geq 1$. Weakly ergodic/mixing system do not follow each of corresponding the features [18].

When $\alpha = 0$ and β is irrational, the map is still ergodic [22], but is never mixing [23]. For the case $\beta = 0$ two situations might occur [16]. If α is a rational number, then the dynamics are pseudo-integrable and confined, whereas for α irrational, the dynamics are found to be weakly ergodic, with the number of y_n taken by a single orbit increasing as $\ln T$ ($0 \leq n < T$). Furthermore, the ultra-slow apparent decay of the correlation function measured for this condition does not provide sufficient evidence of mixing. In recent years, some analytical attempts in order to characterise the map Eq. (1) have been made [24]. Despite this, it has not been possible to prove or reject the mixing property for the Casati-Prosen map although strong indication of a non-mixing property prevails.

3 Results

In this section, we present the numerical results of our study. Namely, we have considered variables X_N and Y_N that are obtained from the addition of x and y variables of map (1),

$$X_N = \sum_{i=1}^N x_i, \quad (2)$$

$$Y_N = \sum_{i=1}^N y_i, \quad (3)$$

that we analyse after detrending and rescaling, $u'_N = (u_N - \langle u_N \rangle) / \sigma_N$ (u renders either X or Y and σ_N is the standard deviation, $\sigma_N^2 = \frac{1}{N} \sum_{i=1}^N u_i^2$). In our survey we have neglected the case $\alpha = 0$ since it destroys the dependence of y on x and we have focussed on the following situations,

$$\text{case I : } \left\{ \begin{array}{l} \alpha = \frac{1}{2} \left[\frac{1}{2} (\sqrt{5} - 1) - e^{-1} \right], \\ \beta = \frac{1}{2} \left[\frac{1}{2} (\sqrt{5} - 1) + e^{-1} \right] \end{array} \right\}, \quad (4)$$

which corresponds to the ergodic and mixing case studied in Refs. [16, 21] and

$$\text{case II : } \left\{ \alpha = \pi^{-\frac{1}{2}}, \beta = 0 \right\}, \quad (5)$$

where the map is weakly ergodic. For each analysis, we have randomly placed a set of initial conditions \mathcal{I} (typically 10^7 elements) within the torus z and we have let the map run. The probability density functions $P(X_N)$ and $P(Y_N)$ are then obtained from these \mathcal{I} initial conditions. Our numerical calculations have been performed using the MATHEMATICATM kernel which assures a symbolic computational procedure. Although analytical considerations in case I are in principle possible, we have skipped them because we have used case I as a benchmark of the peculiar behaviour of case II that we are going to present. It is also worth stating that, for case I, where analytical considerations have been made (or can be made), conditions of strong mixing and (semi)conjugation to a Bernoulli shift are mandatory [9]. These conditions are not verified in our case II.

For case I, as expected from ergodic and mixing properties of map (1), both X_N and Y_N (detrended) approach the Normal distribution [10],

$$G(u_N) = \frac{1}{\sqrt{2\pi\sigma_N^2}} \exp\left[-\frac{1}{2\sigma_N^2}u_N^2\right], \quad (6)$$

as N goes to infinity, see Fig. 1. Moreover, as it occurs for the Lyapunov CLT, σ_N follows the scaling relation,

$$\sigma_N = \sqrt{N}\sigma_1, \quad (7)$$

with $\sigma_1 = \frac{1}{\sqrt{3}}$ as in Fig. 2. In Ref. [16] a similar kind of analysis has been made by considering a cylinder $y \in (-\infty, \infty)$

$$y_n = y_0 + \beta n + \alpha p_n, \quad (8)$$

with $p_n \in \mathbb{Z}$.

We have also verified a skew in our PDFs, for small N , which are not visible in the PDFs of Ref. [16], but might be comprehended according to analytical work made on other types of maps [9, 13]. Explicitly, skewed distributions have *analytically* been found when studying the same problem using the dissipative, fully chaotic and strongly mixing map $x_{t+1} = 1 - 2x_t^2$ [13].

A completely different behaviour is found when case II is analysed. For this case, we have concentrated on X_N , although for Y_N we have obtained the same qualitative results. Instead of distributions reminiscent of a Normal distribution, we have numerically observed probability distributions which are well described by,

$$P(u) \sim |u|^{-\eta-1} \quad (1 \ll u \leq N), \quad (9)$$

with $\eta < 2$ for every value of N analysed, see Tab. 1 and Figs. 6 and 4. The method applied to determine η has been the Meerschärt-Scheffler estimator (see Appendix) [25]. The subsequent application of the Hill estimator [26] has given concordant results.

The upper bound of η we have found ($\eta = 1.80$) imposes that the standard deviation would diverge if the variable $X(Y)$ was defined over the whole interval of real numbers. Since we are treating cases for which N is finite, the support of the resulting PDFs is compact and defined between $-N$ and N for X_N and Y_N . This obviously leads to a finite standard deviation, σ_N , for the cases we have studied. We have verified that σ_N does not follow the scaling relation Eq. (7), see Fig. 3. Instead, a power-law dependence can approximately be given with an exponent close to 0.94 ± 0.02 . In addition, we have observed that the shape of the distribution $P(X_N)$ has strong similarity with the α -stable Lévy distribution

$$\mathcal{L}_\alpha(X_N) = \frac{1}{2\pi} \int_{-\infty}^{+\infty} \exp[-ikX_N - a|k|^\alpha] dk, \quad (10)$$

(($0 < \alpha < 2$)) when plotted in a log-log scale, namely the emergence of an inflexion point before the straight line segment [29]. We must emphasise that this similarity *by no means implies a possible application of Lévy-Gnedenko generalisation of the CLT* which states

Table 1: Values of the maximum value of $P(X_N)_{\max}$, and η parameters characterising PDF Eq. (9) for positive, η_+ , and negative, η_- , branches for each value of N calculated.

N	$P(X_N)_{\max}$	η_+	η_-
10	0.350		
10^2	0.203	1.80	1.81
10^3	0.141	1.57	1.57
2×10^3	0.128	1.52	1.52
4×10^3	0.118	1.47	1.47
8×10^3	0.109	1.41	1.41
1.6×10^4	0.101	1.30	1.29

that, the probability density function of the sum of N variables, each one associated with the same distribution Eq. (9) ($0 < \eta < 2$ and $u \in \Re$) converges in the limit as N goes to infinity to a α -stable Lévy distribution with $\alpha = \eta$. It is easy to verify that the results we report in this manuscript do not follow this theorem because; *i*) x_t and y_t variables are boxed up within intervals from -1 to $+1$ and hence their standard deviations are always finite, *ii*) due to the weak chaotic properties, variables x_t and y_t are not independent at all instants t .

Trying to infer about the scaling behaviour of $P(X_N)_{\max}$ with N , a clear-cut power-law behaviour could not be found as it is visible in Fig. 5.

In the absence of clear power-law behaviour and using the fact that η decreases as N increases, we have tried to extrapolate a value of $\eta(N \rightarrow \infty)$. To this end, inspired by finite-size scaling relations of critical behaviour [27], we have used the following ansatz,

$$\eta(N) = \eta_\infty \left(1 + \frac{1}{1 + cN^\delta} \right). \quad (11)$$

From this, we have obtained $\eta_\infty = 1.02 \pm 0.06$ (see Fig. 4) very close (within error margins) to the exponent of the Lorentzian distribution, $\mathcal{L}_1(X_N)$.

4 Final remarks

In this manuscript we have presented a numerical experiment on the addition of deterministic variables generated by a conservative map, the triangle map of Casati and Prosen [16]. The study has been performed in two different regimes, case I and case II, by iterating the map from a set of initial conditions which have uniformly been placed within interval $[-1, 1)$. In case I, for which the map is ergodic and mixing, the outcoming stable PDF is the Normal distribution for both X_N and Y_N , in perfect accordance with standard theory. In case II, for which the map is weakly ergodic for sure and with apparently no mixing, we have obtained PDFs which are well described by power-laws for large values of the variable. Moreover, the parameter characterising the PDF is smaller than 3 and it

presents a decreasing trend as the number of variables N are augmented³. Our results are to some extent surprising seeing that, notwithstanding the map is weakly ergodic, it fills the phase space as time evolves. Accordingly, it would be expected that Gaussian behaviour would be approached (as in case I) as N increases and not the opposite as we have reported here. In such a scenario of weak chaoticity, the map was expected to present some anomalous (quasi-steady) behaviour before total occupancy of the phase space took place which would imply a crossover to the Normal distribution. This last description is analogous to what has been observed in the fractal dimension, which tends to increase towards the Euclidean dimension, for the case of low-dimensional symplectic maps (see details in Ref. [28]). However, for the case we have studied, the observed increasing departure from the Gaussian distribution with increasing N points to another direction⁴. Last of all, from the ansatz 11, we have extrapolated the value of η when $N \rightarrow \infty$, which has shown to be $\eta_\infty \approx 1$, *i.e.*, the same decay as the Lorentz distribution, which corresponds to a q -Gaussian with $q = 2$ in the non-extensive formalism. In defiance of the different nature of both systems, our result for the Casati-Prosen conservative system has provided a similar qualitative result as obtained in Refs. [13] for the logistic (dissipative) map. In other words, departing from variables with a finite standard deviation that evolve according with a dynamical system in which strongly ergodic and strongly mixing features are not verified, we have been able to define a new variable whose limit distribution (spanning the whole domain of real numbers) has a different attractor than for the Gaussian. Moreover, in our results the mixing property looks to be a crucial element. It is our expectation that, along with results for dissipative dynamical systems, this work should suggest further studies on the introduction of an analytical framework for cases where the Bernoulli shift is not verified.

Acknowledgements

SMDQ would like to thank Prof C. Tsallis for several discussions over several aspects of central limit theory, G. Ruiz for conversations about the application of CLT to deterministic variables, and T. Prosen for his comments on the properties of Eq. (1) and for having provided his work [24] before public disclosure. An acknowledgment is also addressed to Prof T. Cox for the thorough reading and commenting of this manuscript. The work herein presented has benefited from financial support by FCT/MCTES (Portuguese agency) and Marie Curie Fellowship Programme (European Union), and infrastructural support from PRONEX/CNPq (Brazilian agency).

Appendix

The method introduced by Meerschaert and Scheffler [25] is based on the asymptotic limit of the sum of the variables of dataset $\{X_N\}$ under scrutiny. For heavy tail data these asymptotics depend only on the tail index of the probability density function, and not on

³An exponent equal to 3 corresponds to the lower bound for finite second order moment of distributions defined between $-\infty$ and ∞ .

⁴ N can also work as a measure of time.

the exact form of the distribution. Hence, if \mathcal{I} elements of a dataset are identically and (in)dependently distributed, and in addition its probability density function presents an asymptotic behaviour,

$$P(X_N) \sim |X_N|^{-\eta-1}, \quad (|X_N| \rightarrow \infty),$$

it can be proved (Theorem 1 in Ref. [25]) that,

$$\frac{1}{\eta} = \frac{\ln_+ [\sum_{i=1}^{\mathcal{I}} (X_{N,i} - \langle X \rangle)^2]}{2 \ln \mathcal{I}}, \quad (\text{A1})$$

where $\langle X \rangle$ is the simple average $\langle X \rangle = \mathcal{I}^{-1} \sum_{i=1}^{\mathcal{I}} X_{N,i}$ and $\ln_+ [x] \equiv \max \{\ln x, 0\}$.

References

- [1] J. Bernoulli, *Ars Conjectandi* (Basel, 1713)
- [2] A. de Moivre, *The Doctrine of Chances* (Chelsea, New York, 1967)
- [3] P.-S. Laplace, *Théorie Analytique des Probabilités* (Dover, New York 1952)
- [4] A. M. Lyapunov, Bull. Acad. Sci. St. Petersburg **12** (8), 1 (1901)
- [5] P. Lévy, *Théorie de l'addition des variables aléatoires* (Gauthier-Villards, Paris, 1954)
- [6] B. V. Gnedenko, Usp. Mat. Nauk **10**, 115 (1944) (Translation nr. 45, Am. Math. Soc., Providence)
- [7] A. Araujo and E. Guiné, *The Central Limit Theorem for Real and Banach Valued Random Variables* (John Wiley & Sons, New York, 1980)
- [8] P. Hall and C. C. Heyde, *Martingale Limit Theory and Its Application* (Academic Press, New York, 1980)
- [9] C. Beck and G. Roepstorff, Physica A **145**, 1 (1987); C. Beck, J. Stat. Phys. **79**, 875 (1995)
- [10] M.C. Mackey and M. Tyran-Kaminska, Phys. Rep. **422**, 167 (2006)
- [11] C. Tsallis, J. Stat. Phys. **52**, 479 (1988)
- [12] L.G. Moyano, C. Tsallis and M. Gell-Mann, Europhys. Lett. **73**, 813 (2006); S. Umarov, C. Tsallis and S. Steinberg, Milan J. Math. **76**, 307 (2008); S. Umarov, C. Tsallis, M. Gell-Mann and S. Steinberg, arXiv:cond-mat/06006038v2 (pre-print, 2006); S. Umarov, C. Tsallis, M. Gell-Mann and S. Steinberg, arXiv:cond-mat/06006040v2 (preprint, 2006); S. Umarov, C. Tsallis, Phys. Lett. A **372**, 4874 (2008); F. Baldovin and A. Stella, Phys. Rev. E **75**, 020101(R) (2007); C. Vignat and A. Plastino, J. Phys. A: Math. Theor. **40**, F969 (2007); S. Umarov and C. Tsallis, AIP Conf. Proc. **965**, 34-42 (2007); H.J. Hilhorst and G. Schehr, J. Stat.

- Mech. P06003 (2007); A. Rodríguez, V. Schwämmle, C. Tsallis, J. Stat. Mech. P09006 (2008); S. Umarov and S.M.D. Queiros, [arXiv:0802.0264\[cond-mat.stat-mech\]](#) (pre-print,2008);
- [13] U. Tirnakli, C. Beck and C. Tsallis, Phys. Rev. E **75**, 040106 (2007), *idem*, [arXiv:0802.1138v1 \[cond-mat.stat-mech\]](#) (preprint, 2008)
 - [14] G. Ruiz, S.M. Duarte Queirós and C. Tsallis (unpublished, 2007); G. Ruiz and C. Tsallis, Eur. Phys. J. B (in press, 2009) [arXiv:0802.1138v1 \[cond-mat.stat-mech\]](#)
 - [15] A. Pluchino, A. Rapisarda and C. Tsallis, EPL **80**, 26002 (2007), A. Figueiredo, T.M. da Rocha Filho, and M.A. Amato, EPL **83**, 30011 (2008); A. Pluchino, A. Rapisarda and C. Tsallis, Physica A **387**, 3121 (2008)
 - [16] G. Casati and T. Prosen, Phys. Rev. Lett. **85**, 4261 (2000)
 - [17] G. Casati and T. Prosen, Phys. Rev. Lett. **83**, 4729 (1999)
 - [18] A. Katok, B. Hasselblatt, *Introduction to the modern theory of dynamical systems* (Cambridge University Press, Cambridge, 1995)
 - [19] F. Baldovin and A. Robledo, Phys. Rev. E **69**, 045202 (2004); A. Robledo, Physica A **370**, 449 (2006)
 - [20] C. Tsallis, A.R. Plastino and W.-M. Zheng, Chaos, Solitons & Fractals **8**, 885 (1997)
 - [21] G. Casati, C. Tsallis and F. Baldovin, Europhys. Lett. **72**, 355 (2005)
 - [22] H. Furstenberg, Am. J. Math. **83**, 573 (1961)
 - [23] I. P. Cornfeld, S.V. Fomin, and Ya.G. Sinai, *Ergodic Theory* (Springer-Verlag, New York, 1982).
 - [24] F. Christiansen and A. Politi, Nonlinearity **9**, 1623 (1996); M. Horvat, M. Degli Esposti, S. Isola, T. Prosen and L. Bunimovich, Physica D **238**, 395 (2009)
 - [25] M.M. Meerschaert and H.-P. Scheffer, J. Stat. Plan. Infer. **71**, 19 (1998)
 - [26] B. Hill, Ann. Statist. **3**, 1163 (1975)
 - [27] H.J. Herrmann, Phys. Rep. **136**, 153 (1986)
 - [28] F. Baldovin. E. Brigatti and C. Tsallis, Phys. Lett. A **320**, 254 (2004)
 - [29] C. Tsallis and S.M. Duarte Queirós, AIP Conf. Proc. **965**, 8 (2007)
 - [30] J. McCulloch, J. Business Econ. Statist. **15**, 74 (1997)

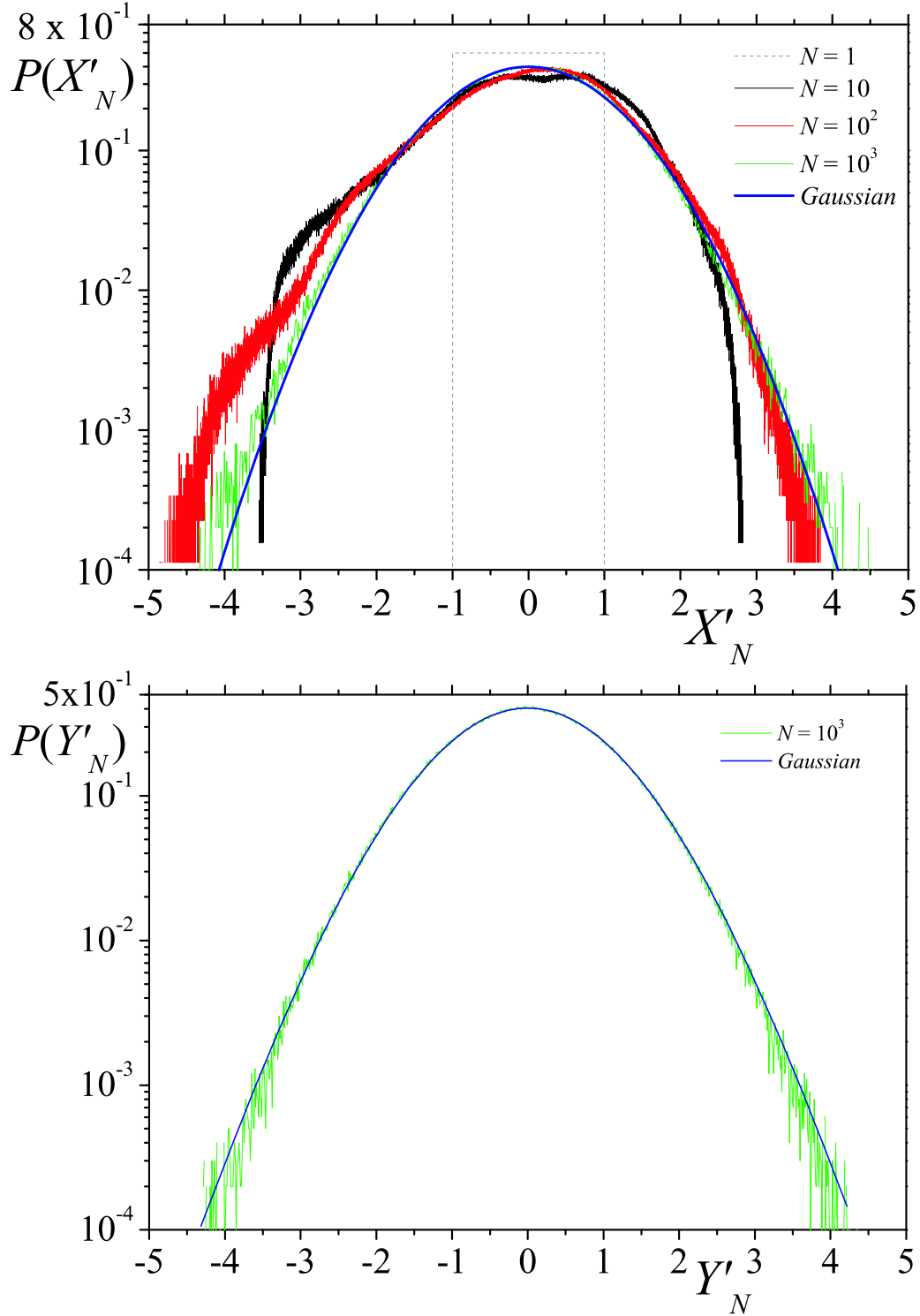


Figure 1: Upper panel: Probability density function $P(X'_N)$ vs X'_N for scaled variables $X'_N \equiv X_N - \langle X_N \rangle / \sigma_N$, obtained in case I where $\langle X_N \rangle$ represents the average of X_N [on log-linear scale]. Lower panel: The same as the upper panel, but for variable Y_N . In both panels the line labelled *Gaussian* corresponds to Eq. (6) with $\sigma_N = 1$.

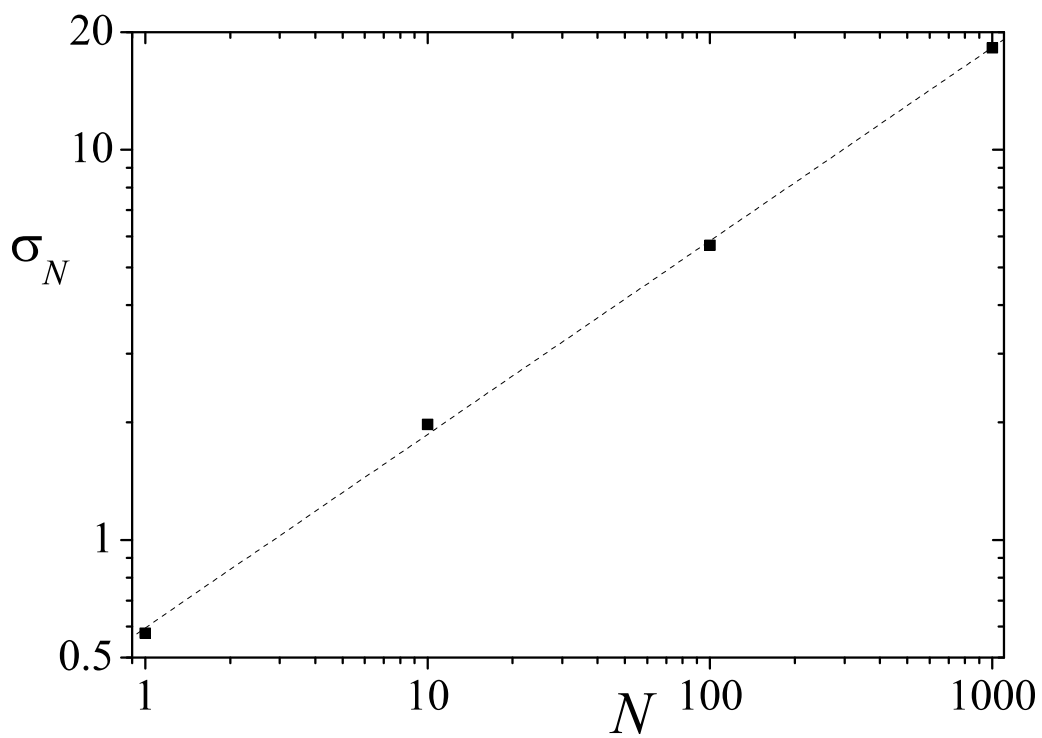


Figure 2: Standard deviation, σ_N , of X_N vs. N for case I [on log-log scale]. The fitted straight line has a slope of 0.49 ± 0.01 .

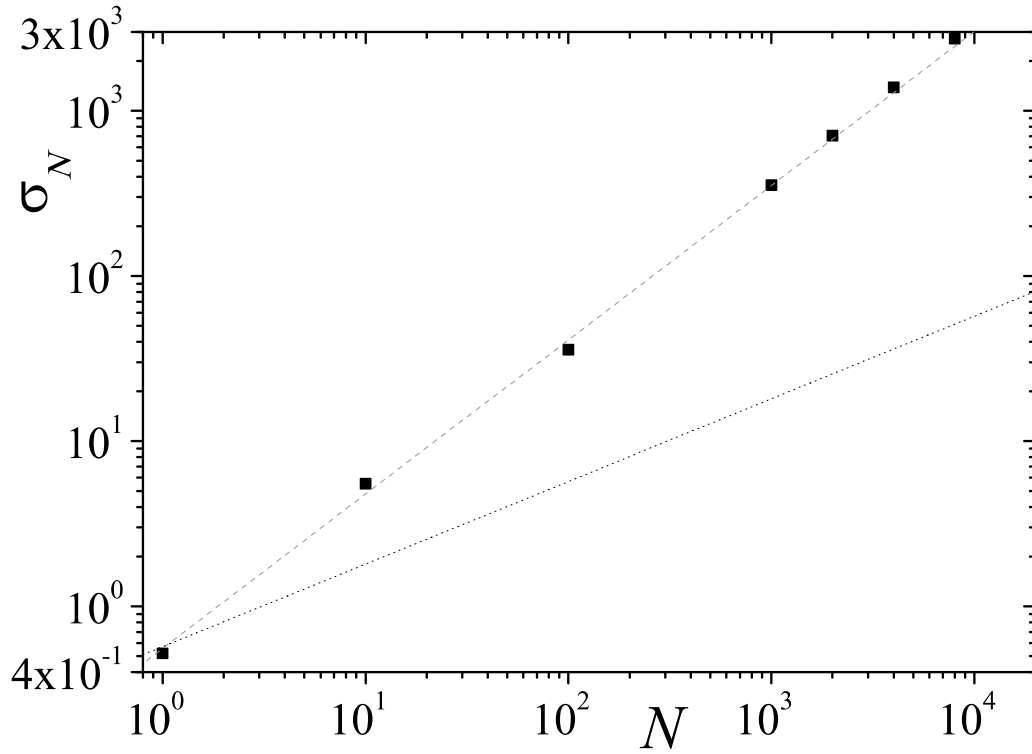


Figure 3: Standard deviation σ_N *vs* N of X_N obtained from map (1) [on log-log scale]. The dotted line corresponds to Eq. 7 and the grey dashed line has slope 0.94 ± 0.02 corresponding to the best linear fit on this particular scale.

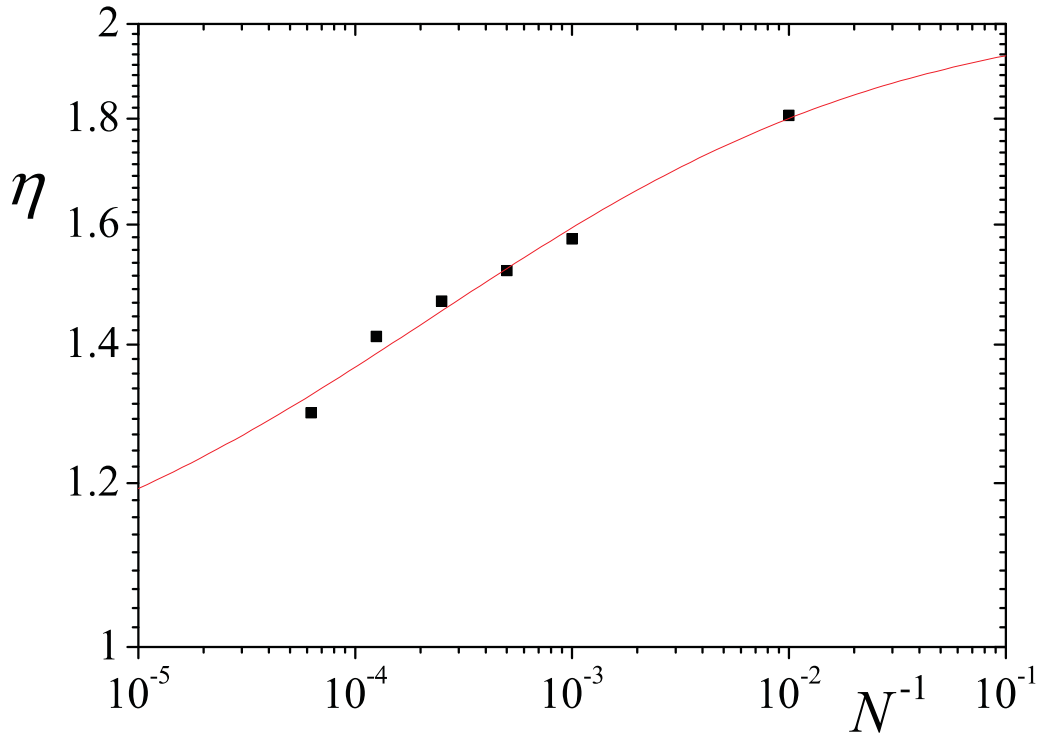


Figure 4: Values of the exponent for positive side, η_+ , vs. N^{-1} [on log-log scale]. The line represents a numerical adjustment for Eq. (11) with $\eta_\infty = 1.02$, $c = 0.049$, and $\delta = 0.40$ ($\chi^2 = 6.9 \times 10^{-4}$ and $R^2 = 0.986$).

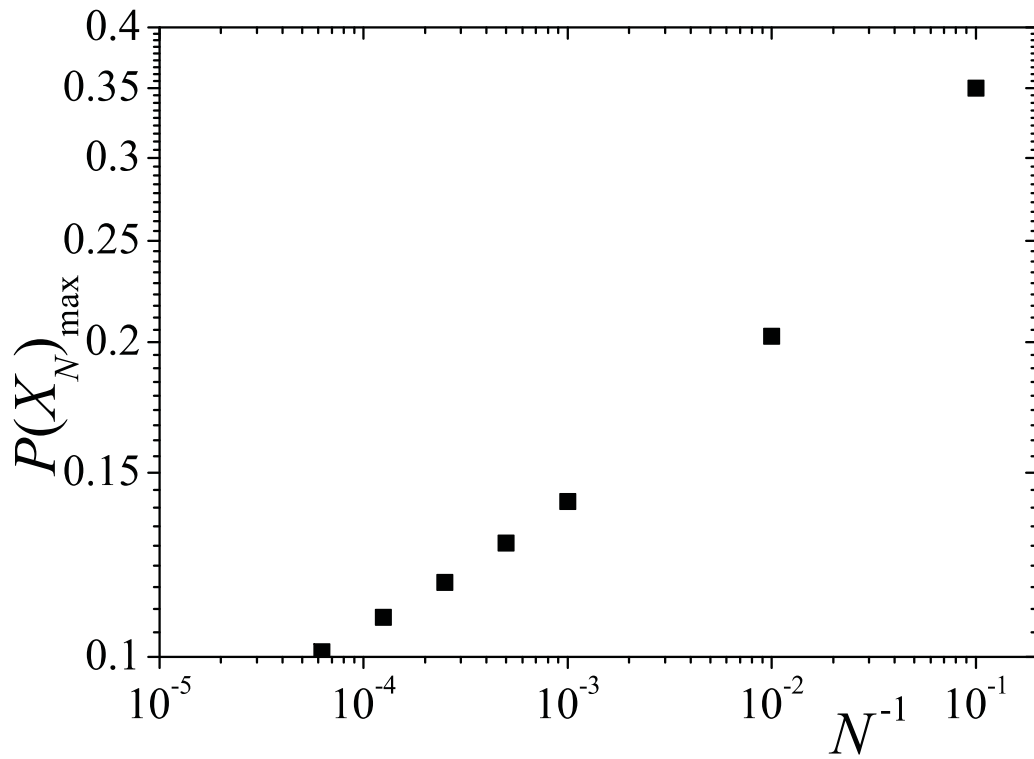


Figure 5: Maximum value $P(X_N)_{\max}$ vs. N^{-1} according to the values of Table 1 [on log-log scale].

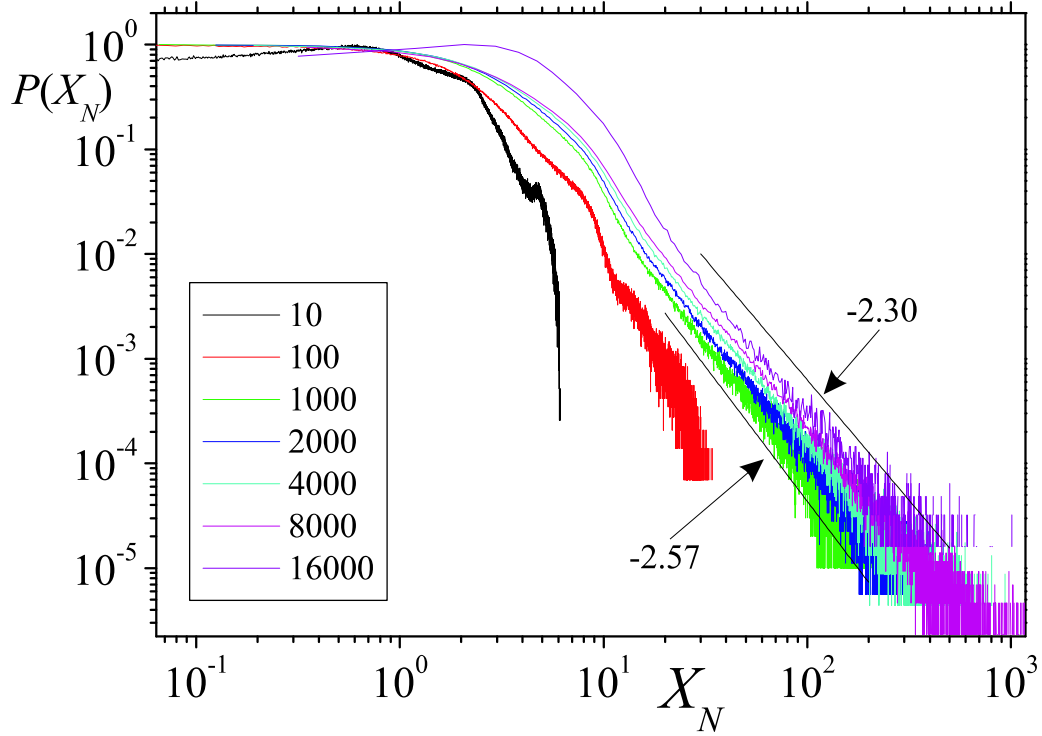


Figure 6: Probability density function $P'(X_N) = \frac{P(X_N)}{P(X_N)_{\max}}$ vs X_N [in log-log scale]. The number of initial conditions (points used to construct PDFs) is 10^7 except for $N = 8000$ (7.5×10^6 points) and $N = 16000$ (7×10^5 points). The power-law decay is evident for large X_N . The two straight lines have slopes $-(\eta_+ + 1)$ with η the exponent for $N = 1000$ and $N = 16000$ (see Table 1).